Field-Circuit Co-Simulation of the Marx Generator

Qian Xu[1], He Jiang[2], Yi Huang[3], Jiafeng Zhou[4], Chaoyun Song and Lei Xing
[1] qian.xu@liv.ac.uk
[2] jheriver@liv.ac.uk
[3] yi.huang@liv.ac.uk
[4] jiafeng.zhou@liv.ac.uk
Department of Electrical Engineering and Electronics, University of Liverpool, Liverpool, UK

***Abstract*— A full wave field-circuit co-simulation method is employed to characterise the time domain behaviour of the Marx generator. Radiation and conduction effects are fully considered. Results from the co-simulation and the circuit simulation are compared; it can be found that the field-circuit co-simulation provides complete information of the system which includes the radiation effect and the mutual coupling in space. The radiated field strength is important when designing the shielding room which is used to protect the measurement instruments in practice.**

***Index Terms*—field-circuit co-simulation, computer simulation, Marx generator.**

I. INTRODUCTION

The Marx generator is widely used in high voltage pulse generation, first described by Erwin Otto Marx in 1924. The basic principle is to charge the capacitors in parallel and then discharge them in series.

Traditionally, in the design procedure of the Marx generator, the circuit model is used to simulate it [1-4]. However, the circuit model is not enough when considering the radiation and mutual coupling effect of the whole system. Full wave method such as FIT (Finite Integration Technique) has been used to simulate the structure, but the coupling is in one direction: the structure is excited using a given signal which means the coupling from the circuit to radiation is considered, but the signal coupled from the field to circuit is ignored [5,6]. From physical point of view, this procedure is not self-consistent, when dealing with a more delicate design this method may not be accurate enough.

The bi-directional simulation which considers all couplings in the system can be regarded as a self-consistent way to simulate this kind of problem. This technique has been applied to the ESD (Electrostatic Discharge) [7] and lightning simulation [8], however, no report has been found for the Marx generator simulation using this method which is the major work of this paper. By using this method, the results from radiation and conduction are obtained simultaneously; the radiated electric field strength is important when designing a shielding room to protect the measurement instruments in such a high pulse field environment. Thus, a safety margin can be evaluated before actually deploy the measurement system.

In this paper, a 4-stage Marx generator is analysed, results from circuit simulation are given in the next section, field-circuit co-simulation is employed in Section III, both charging and discharging process are simulated, results in both time domain and frequency domain are analysed. Discussions and conclusions are given in the final section.

II. CIRCUIT SIMULATION

The 4-stage Marx generator is shown in Fig. 1(a). In the experiment, we found that the break down voltage for each stage is 15 kV. The shielding room used to protect the measurement instrument from the radiation is shown in Fig. 1(b). The schematic of the 4-stage Marx generator is given in Fig. 2, the element values are listed in Table I. The output signal is filtered by the capacitor *Cload* and decays exponentially.

It is well known that when the first air gap breaks down, the others will break down automatically in sequence. The capacitors are connected in series and discharge as shown in Fig. 3. If the charging voltage is 15 kV, ideally it will create an output voltage of $-15 \times 4 = -60$ kV. However, in practice, because of the radiation, imperfect switch, conduction loss, *etc*. the output voltage is smaller than the ideal value.

The CST (Computer Simulation Technology) Design Studio is used to simulate this ideal discharging circuit as shown in Fig. 4. The voltage controlled switch is used to trigger the discharge. The resistors *Rcharge* can be ignored, since it is in MΩ and much larger than the *Rtail* and *Rload*. The initial condition of the capacitor is set as fully charged with voltage -60 kV. Three probes are used to record the voltage signal. The switch is triggered on by using a step signal at 800 ns.

The simulation time for this scenario is very short and finished in 3 secs. The output voltage signals at the probes are shown in Fig. 5. These results are compared with that from the field-circuit co-simulation in the next part.

TABLE I. ELEMENT VALUES

Name	Value	Unit
Rcharge	6	MΩ
Ccharge	0.02	uF
Rfront	10	Ω
Rtail	100	kΩ
Rload	60	Ω
Cload	500	pF
Rdv1	100	kΩ
Rdv2	60	Ω

III. FIELD-CIRCUIT CO-SIMULATION

The CST Microwave Studio and Design Studio are connected together to realise the field-circuit co-simulation. In each time step the field components **E**, **H** and the circuit components *V* and *I* are updated synchronously. The structure is shown in Fig. 6. The capacitors, resistors and wires are modelled as the lumped elements (Fig. 6(b)); the air gaps are connected using ports which will be triggered in the CST Design Studio (Fig. 8). The boundary condition for the ground plane is set as PEC (Perfect Electric Conductor); the others are set as PML (Perfect Matched Layer) to emulate the free space.

A. Charging Process

Since the charging resistor *Rcharge* is very large and the charging time is in seconds, it is impossible to simulate the charging process directly in the field-circuit co-simulation, as the time step is determined by the smallest mesh size and normally in nanoseconds. To avoid this long charging time in simulation, an extra port is used to charge the capacitors directly (Fig. 7). After the capacitors are fully charged, the ports will become isolated and will not affect the discharging process which is shown in Fig. 8. The port 9 will be used to control the switch to charge the capacitors, after the capacitors are fully charged; the switches will be set as off. The voltage curves in the charging process of all the capacitors are shown in Fig. 9. As can be seen, all the capacitors are charged simultaneously and reach to 15 kV at around 300 ns, it should be noted that the overshoot is due to the inductance of the wires used to connect the components which is easy to be ignored in the circuit-only simulation.

The field distribution of the charging process is shown in Fig. 10. After the capacitors are fully charged, at 800 ns the discharging process will be triggered by port 1-8 in Fig. 8. The E-field distribution at 800 ns in Fig. 10(b) can be regarded as the initial condition for the discharging process.

B. Discharging Process

Because the air gaps break down in sequence in discharging process, the switches in Fig. 8 are triggered in sequence with 2 ns delay time (Fig.11). In practice, there is a metallic plane between the electrodes of the air gap (Fig. 7), each air gap is modelled with 2 discharging ports, these makes 8 ports in total. Far-field probes at 1 m distance are used to record the radiated field shown in Fig. 12.

The simulation is finished in 20 hrs 5 mins (752,106 time steps) on a PC, the mesh no. is 380,640 (hexahedra) and the memory consumption is 1.2 GB. The voltage signal at *Rload* and *Rtail* are shown in Fig. 13, and are compared with the results from the circuit-only simulation (Fig. 5). It can be seen that it agrees well with each other in the full time scale, but the circuit simulation ignores all the distributed effect (mutual coupling, radiation, *etc*.) and is smoother. Especially at the beginning of the discharging (Fig. 13(b)), the result from the circuit-only simulation provides limited information; the high frequency component of the signal is ignored. The radiated E-field at 1 m distance is shown in Fig. 14. It was found that the dominate component of the E-field is the vertical polarisation and the magnitude of the E-field decays exponentially (Fig. 14(b)), the corresponding spectrum is also given in Fig. 14(c), which shows that most of the radiated energy is around 200 MHz. The E-field distribution at different time steps is given in Fig. 15 which gives a direct understanding of the field propagation in the discharging process. It can be seen that the air gaps break down in sequence as shown in Fig. 15(a) ~ (d) from top to bottom.

IV. CONCLUSIONS

A system simulation of the Marx generator has been studied which includes all distributed effect (mutual coupling, radiation, *etc*.); this field-circuit co-simulation is bi-directional and self-consistent, the radiation from the circuit and the interference from the radiated field to the circuit are considered. The transient radiated field has been obtained, and provides important information before measurement, a safety margin for the shielding effectiveness of the screened room used to protect the instruments can be evaluated. We believe this field-circuit co-simulation method provides detailed physical insight when designing delicate and sophisticated Marx generator, especially in the area of EMP (Electromagnetic Pulse) generation and protection.

It should be noted that the field-circuit co-simulation is time consuming, since the maximum time step is restricted by the smallest mesh size of the 3D model, another thing should be carefully treated is that, before simulation, the frequency range of the signal should be estimated to ensure the signal generated during the simulation is in the pre-set frequency range, otherwise the simulation may become unstable. In this paper, the mesh is stable up to at least 2 GHz, and it can be seen in Fig. 14(c) that at 2 GHz, the signal strength is 60 dB smaller than the peak value which means the frequency range should be wide enough for this case.

Future work may include more detailed research in the modelling of the air gap. In this paper, constant resistance and parasitic capacitance are used when the circuit is switched on. In reality, the behaviour of the switch is nonlinear and time dependent [9-11], more complex model may need and the results comparison between the measurement and simulation may include.

REFERENCES

[1] Y. E. Kolyada, O. N. Bulanchuk and V. I. Fedun, "Numerical simulation of the Marx-generator behavior on nonlinear load-high-current vaccum diode," Vopr. At. Nauki Teh., Âd.-Fiz. Issled. 5 pp.27-29, 2001.

[2] R. Sheeba, M. Jayaraju, T. K. N. Shanavas, "Simulation of impulse voltage generator and impulse testing of insulator using MATLAB Simulink," Word Journal of Modelling and Simulaiton, vol. 8, no. 4, pp. 302-209, 2012.

[3] J. R. Mayes and C. W. Hatfield, "Development of a sequentially switched Marx generator for HPM loads," Pulsed Power Conference, 2009. PPC '09. IEEE, pp.934-937, Jun. 2009.

[4] M. S. Kamarudin, E. Sulaiman, M. Z. Ahmad, S. A. Zulkifli and A. F. Othman, "Impulse generator and lighting characteristics simulation using Orcad PSpice software," Proceedings of EnCon 2008, pp. 1032-1037, Dec., Malaysia, 2008.

[5] T. A. Holt, M. G. Mayes, M. B. Lara and J. R. Mayes, "A Marx generator driven impulse radiating antenna," Pulsed Power Conference, 2009. PPC '09. IEEE, pp.489-494, Jun. 2009.

[6] S. V. Tewari, S. B. Umbarkar, R. Agarwal, P. C. Saroj, A. Sharma, K. C. Mittal and H. A. Mangalvedekar, "Development and analysis of PFN based compact Marx generator using finite integration technique for an antenna load," IEEE Trans. on Plasma Science, vol. 41, no. 10, pp. 2684-2690. Oct., 2013.

[7] D. Liu, A. Nandy, D. Pommerenke, S. J. Kwon and K. H. Kim, "Full wave model for simulating a noiseken ESD generator," IEEE International Symposium on Electromagnetic Compatibility, EMC 2009, pp.334-339, Aug. 2009.

[8] E. Kowalczuk, "Exploring lightning susceptibility of composite materials and cable harnesses in aircraft through electromagnetic simulation," IET Seminar on Lightning Protection for Aircraft Components, pp.1-26, Dec. 2013.

[9] R. Montaño, M. Becerra, V. Cooray, M. Rahman and P. Liyanage, "Resistance of spark channels," IEEE Trans. on Plasma Science, vol. 34, no. 5, pp. 1610-1619, Oct. 2006.

[10] S. Bindu, H. A. Mangalvedekar, S. Umbarkar, A. Sharma, D. P. Chakravarti, P. C. Saroj and K. C. Mittal, "Modelling of a spark gap switch," IEEE 10th International Conference on the Properties and Applications of Dielectric Materials (ICPADM), pp.1-4, Jul. 2012.

[11] S. Bindu, M. Parekh, H. A. Mangalvedekar, A. Sharma and D. P. Chakravarthy, "Modelling and analysis of high pressure peaking switch," Journal of Physics Conf. Series **377** 012098, 2012.

(a) (b)

Fig. 1. (a) 4-stage Marx generator. (b) the shielding room used to protect the measurement instruments.

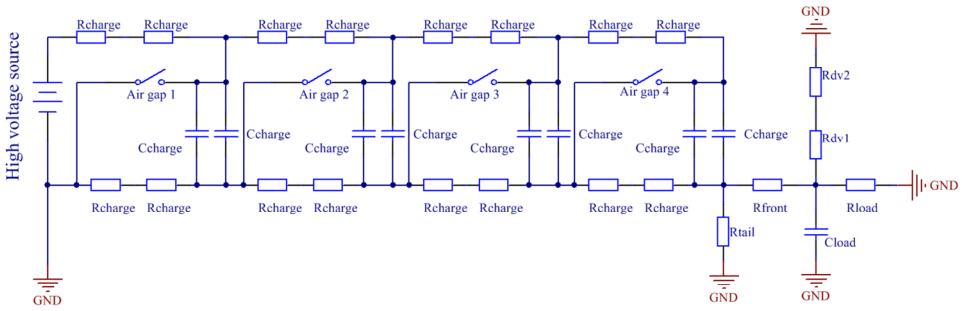

Fig. 2. The circuit of the 4-stage Marx generator.

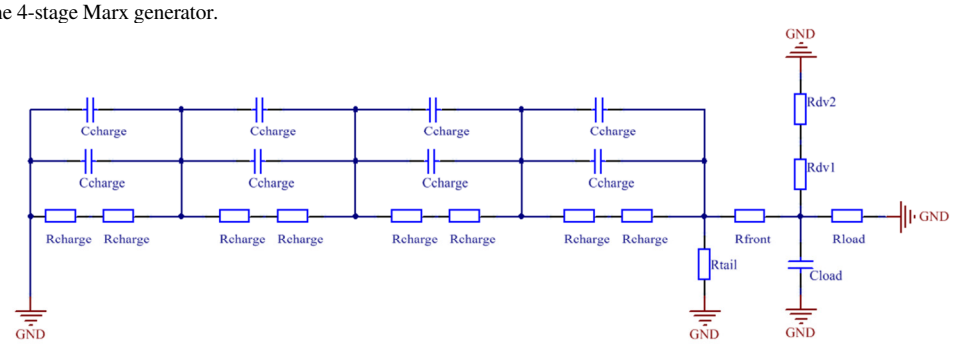

Fig. 3. Discharge equivalent circuit of the Marx generator.

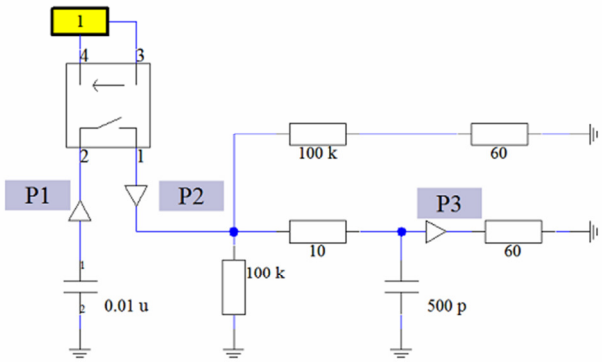

Fig. 4. Discharge circuit simulation in CST Design Studio.

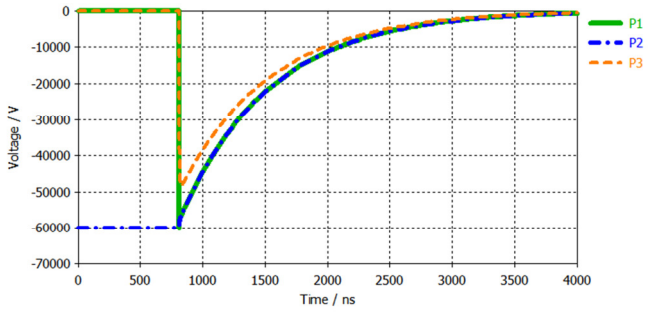

Fig. 5. Discharge voltage signal at defined probes.

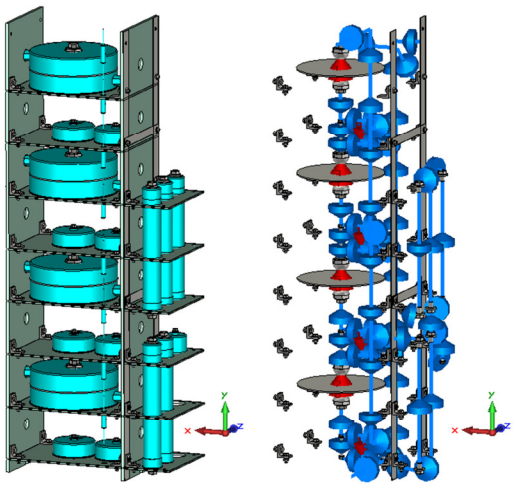

(a) (b)

Fig. 6. (a) 3D model in CST Microwave Studio (b) Lumped elements, ports and wires.

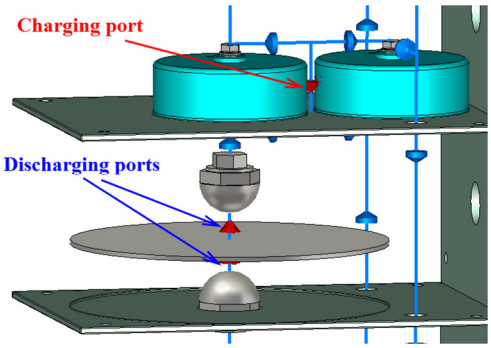

Fig. 7. Zoom in view of each stage.

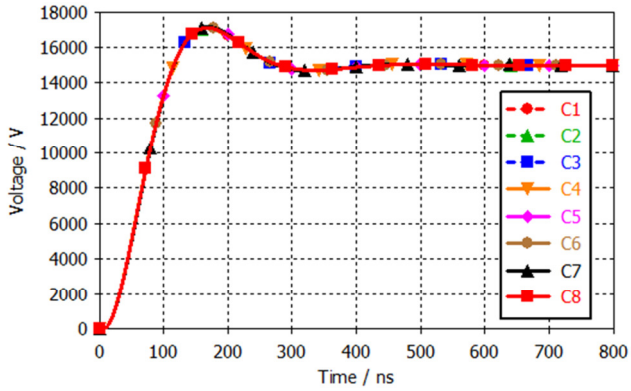

Fig. 9. Voltage charge curves of all the capacitors.

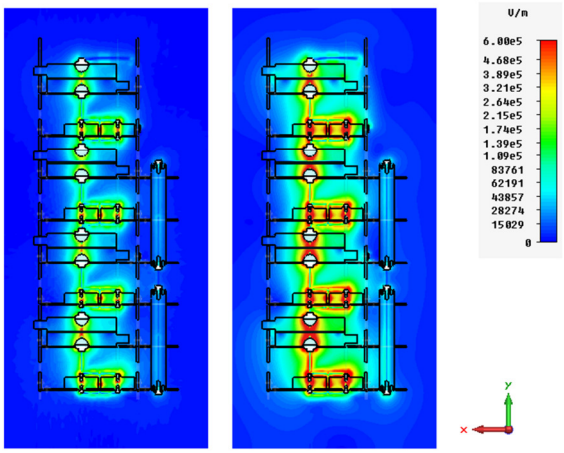

(a) (b)

Fig. 10. E-field distribution in charging process (a) E-field at 50 ns, (b) E-field at 800 ns.

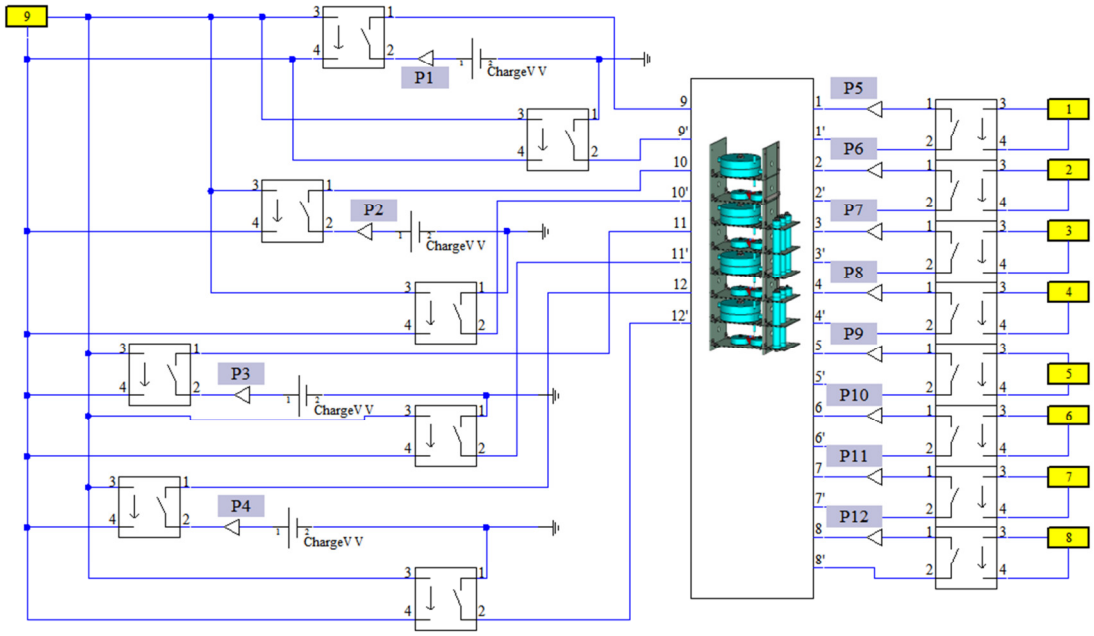

Fig. 8. The circuit used to control the charge and discharge.

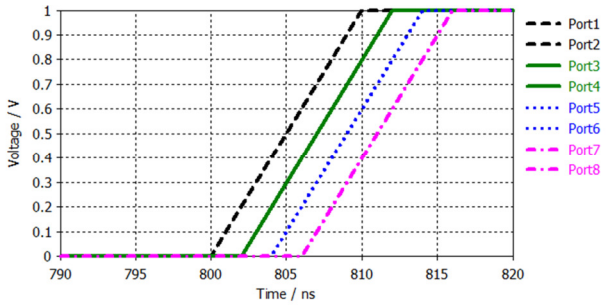

Fig. 11. Port signals used to trigger the capacitor discharge.

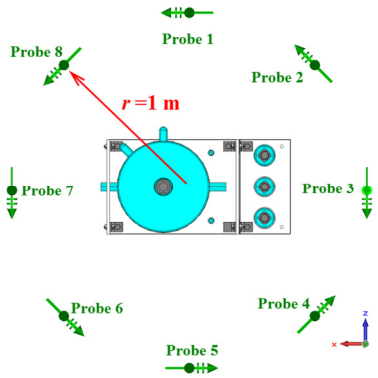

Fig. 12. Far-field probes used to record the radiated field (1 m).

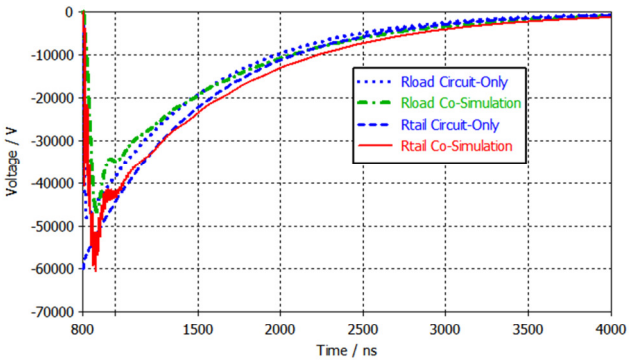

(a)

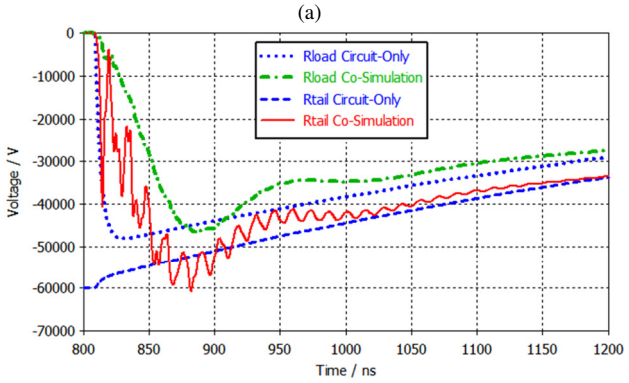

(b)

Fig. 13. Voltage discharge curves comparison. (a) full time scale, (b) zoom in view.

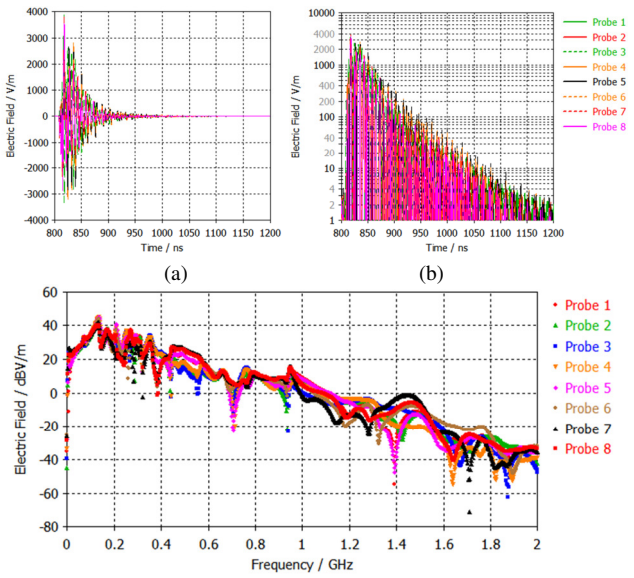

(a) (b)

(c)

Fig. 14. Radiated E-field at probes. (a) full time scale, (b) log scale, (c) spectrum.

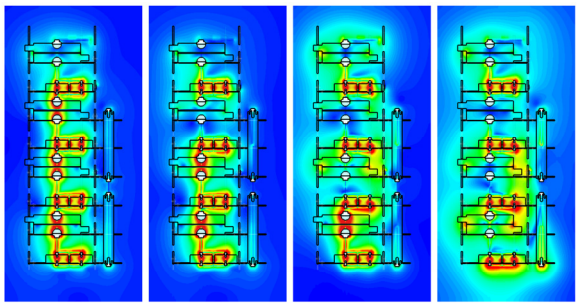

(a) (b) (c) (d)

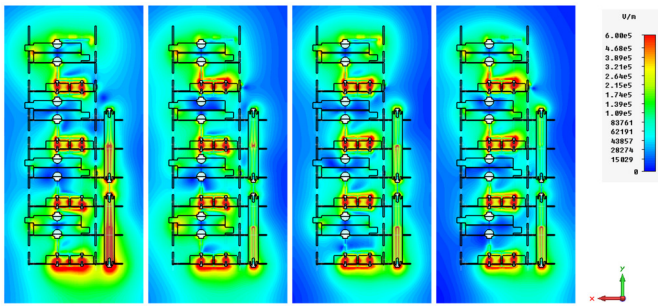

(e) (f) (g) (h)

Fig. 15. E-field distribution in discharging process (a) 807 ns, (b) 809 ns, (c) 811 ns, (d) 813 ns, (e) 815 ns, (f) 817 ns (g) 819 ns, (h) 821 ns.